Three-Phase D-STATCOM with Digital Current Control Strategy in abc-Reference Frame

Tiago Davi Curi Busarello
Depart. Control, Automation and Computation Engineering
Federal University of Santa Catarina - UFSC
Blumenau, Brazil
tiago.busarello@ufsc.br

Kamran Zeb
School of Electrical Engineering; School of Electrical Engineering and Computer Science.
Pusan National University; National University of Sciences and Technology.
Busan, South Korea; Islamabad, Pakistan
kamran.zeb@pusan.ac.kr

Muhammad Asim Sarwar
Department Of Electrical Engineering, Sukkur IBA University, Pakistan
asimsarwar.be17@iba-suk.edu.pk

Hee Je Kim
School of Electrical Engineering
Pusan National University
Busan, South Korea
heeje@pusan.ac.kr

***Abstract*— This paper proposes a Three-phase D-STATCOM with digital current control strategy in abc-reference frame. The proposal D-STATCOM does not use a PLL and the reactive power is transferred to the grid through controlling the D-STATCOM output current. The current controller has one zero and two poles. This type of controller is also known as Type-2 controller. The procedure to tune the controller is explained. The Conservative Power Theory (CPT) is used to compute the reactive power of the loads. A case study shows the behavior of the D-STACOM during initialization, during load transitions and during steady-state conditions. The results show the efficacy of the proposed D-STATCOM.**

Keywords—D-STATCOM, abc reference frame, current control, inverter, reactive power.

I. INTRODUCTION

Reactive power circulation in electric system is under concern since Steinmetz first identifies such power on his apparatus in the nineteenth century [1]. So far, several techniques were developed in order to compensate reactive power produced or consumed by loads. Initially, passive solutions like capacitor bank and Passive Tuned Filter (PTF) addressed pretty well such purpose. However, ageing and temperature cause parameter variations and, consequently, deteriorate the efficacy of these filters. Additionally, capacitors and PTF are usually designed for known loads. The inclusion or removal of load may cause a mismatch in the reactive power between the compensator and the loads.

Solution to overcome these issues were gradually developed along the decades. Examples the Reactive Thyristor Converter (RTC) and Synchronous Motor (SM). SM can handle reactive power by adjusting the field current. On the other hand, RTC is a thyristor-controlled converter and allow variation in the voltage across its capacitor or inductor. As a result, the reactive power produced or consumed by the RTC can vary according to firing angles of the thyristors. The RTC has the drawback of producing high current and voltage derivates, irradiating electromagnetic pollution.

Despite the fact of the drawbacks afore-mentioned, passive solutions, the RTC and SM are still a current choice for reactive power compensation due to mainly their low initial cost and robustness.

With the electronic advancement, reactive power compensators based on IGBT-converter become common. Different topologies allow the conceiving of compensators with a variety of features, such as voltage and frequency regulation, operation at high switching frequency, soft switching, power loss reduction and low volume output filters. Afterwards, reactive power compensation of loads appeared as an ancillary service of Distribute Generators (DG). This means that a DG injecting its available active power and simultaneously injecting reactive power.

One of the most common solution based on IGBT-converter is the Three-Phase Distributed Static Compensator (D-STATCOM) [2]–[4]. The D-STATCOM is able to compensate reactive power at the point where it is connected. Regarding control strategies, D-STATCOM is preferable controlled in dq-rotating reference frame [5]–[24]. The reason for using dq-rotating reference frame is because Proportional-Integrator (PI) controllers may be employed to control AC variables. The D-STACOM can be controlled in current or voltage. In case the D-STATCOM is controlled in current, its output current is 90-degree shifted related to the Point of Common Coupling (PCC) and such a current transfer the reactive energy from the D-STATCOM to the grid. In voltage control mode, the D-STATCOM injects reactive power through varying the voltage or frequency at the PCC. However, in voltage mode, the behavior of the D-STATCOM is strongly dependent on the grid impedance. Control strategies of D-STATCOM usually employ the PQ Theory [25] to compute the amount of reactive power the D-STATCOM will handle.

Controlling a STATCOM using the dq-rotating reference frame has some drawbacks. The most notorious is the dependence of a Phase-Locked Loop (PLL) and is efficacy to track the phase grid even under the presence of disturbances and distortions. In case the PLL is not sufficient, the dq transformation is compromised and the whole behavior of the STATCOM is deteriorated.

This paper proposes a Three-phase D-STATCOM with digital current control strategy in abc-reference frame. The proposal D-STATCOM does not use a PLL and the reactive power is transferred to the grid through controlling the D-STATCOM output current. The current controller has one zero and two poles. This type of controller is also known as Type-2 controller. The procedure to tune the controller is explained. The Conservative Power Theory (CPT) [26]–[30] is used to compute the reactive power of the loads. This theory is being broadly used in power electronics applications especially those involving smart-grids. A case study shows the

The authors are grateful to National Council for Scientific and Technological Development – CNPq (grant 421281/2016-2).

978-1-7281-4970-7/20/$31.00 ©2020 IEEE

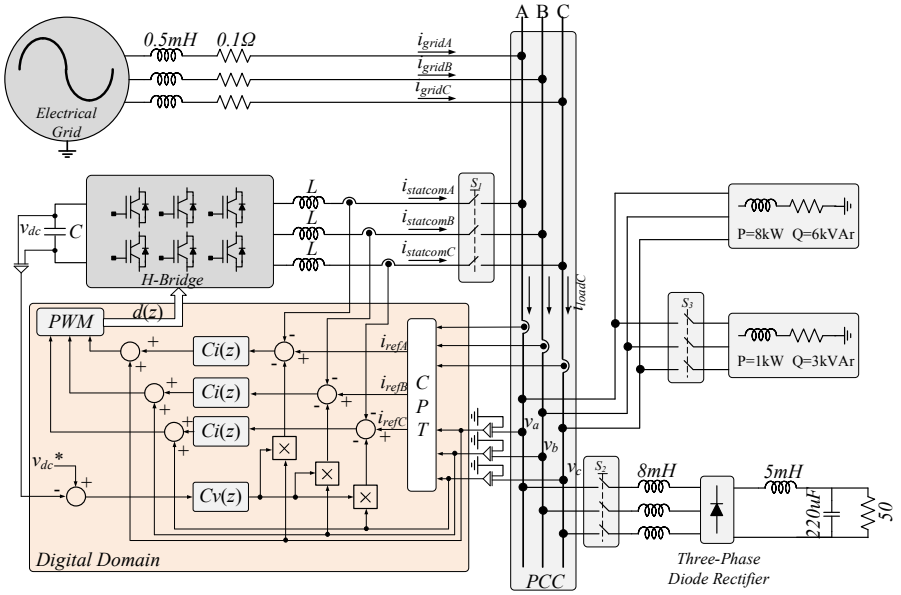

Fig. 1. The system under study as well as the control strategy.

behavior of the D-STACOM during initialization, during load transitions and during steady-state conditions. The results show the efficacy of the proposed D-STATCOM.

II. System Perspective

Fig. 1 presents the system under study as well as the control strategy. The system is a three-phase electric grid with linear and nonlinear loads. The D-STATCOM is a three-phase inverter with RL output filter and it is connected at the PCC The resistance R in output filter represents the cooper losses of the inductor L and it is omitted in the figure. The D-STATCOM is controlled in current mode. Three switches S1, S2 and S3 are presented in the system in order to show transitory behavior of the D-STACOM under some connections. The D-STATCOM and the nonlinear load have pre-charge schemes, not shown in the figure.

About the control strategy, the figure shows its algorithm. The control strategy runs in abc-reference frame. The variable used on the control strategy are measured through current and voltage sensors and they are: the D-STATCOM output current, the load current and the PCC voltage. Notice that the load current comprises all loads connected at the PCC. In the occurrence of a connection of a new load at the PCC, the connection must be beneath the current sensors that measures the load current. All the control strategy is within a digital domain. It means that each measure variable passes through a sampler with zero order holder (not shown in the figure).

The load current and the PCC voltage are sent to the CPT block, which in turn computes the amount of reactive power of the loads and also produces the reference current for the D-STATCOM. The reference current is compared to the D-STATCOM output current and the resulted single passes thought the current controller. The current controller is made with a zero and two poles. Throughout this paper, the current controller is going to be called Type-2 controller. The output signal of the controller is summed with the PCC voltage. This summation acts as a feedforward action of the PCC voltage. The DC-link voltage of the D-STATCOM is controlled through a PI controller and its output signal is subtracted from the current reference. PWM is used to produce the pulse signals of the transistor of the D-STACOM. Finally, it is important to highlight that the control strategy does not use a PLL. The CPT produces the current reference already phase-shifted related to the grid voltage. The CPT also does not use a PLL neither matrix transformation like those found in PQ and dq-rotating reference frame.

III. Designing the Digiital Current Controller

This section presents the design procedure to tune the current controller. The procedure is going to be presented for phase A. Since the control strategy is in abc-reference frame, the procedure for phase A is valid also for phases B and C. Actually, the controller designed for phase A is just replicated for phase B. The control strategy is a classical closed-loop mesh.

The principle of designing the digital current controller is first design an analog controller and later discretize it through the Backward-Euler approximation. For most of applications, this procedure is sufficient to present a satisfactory controller response. An alternative to this approach would be to follow the steps in chapter 4 of [31]. Nevertheless, as stated, the Bacward-Euller approximation may be verified at a first moment. In case of satisfactory controller response, such approximation can be employed.

The procedure to tune the controller begins knowing, or obtaining, the transfer function which relates the output current and the duty-cycle of the D-STATCOM. According to variable definition in Fig. 1, the transfer function is given by (1).

$$G_i(s) = \frac{i_{stacomA}(s)}{d_a(s)} = \frac{v_{dc}}{sL+R} \quad (1)$$

The open-loop transfer function without the controller is given by (2).

$$OLTF_u(s) = G_i(s)PWM(s)H_i(s) \quad (2)$$

Where *PWM(s)* and *Hi(s)* are the transfer functions of the PWM and the current sensor. The *PWM(s)* is equal to one and the *Hi(s)* is equal to the current sensor gain.

The transfer function of the Type-2 controller is given by (3).

$$C_i(s) = \frac{1+sR_2C_1}{sR_1(sR_2C_1C_2+C_1+C_2)} \quad (3)$$

By defining the desired phase margin φ_d and the desired cut-off frequency f_c, the parameters of (3) are obtained through the following equations. Descriptions of these equations are given in the next paragraph.

$$Phase_{fc} = \angle OLTF_u(f_c) \quad (4)$$

$$G_{dB} = |OLTF_u(f_c)| \quad (5)$$

$$G_{real} = 10^{\frac{|G_{db}|}{20}} \quad (6)$$

$$\alpha = \varphi_d - Phase_{fc} - 90° \quad (7)$$

$$k = tan\left(\frac{\alpha}{2} + 45°\right) \quad (8)$$

$$R_1 = \frac{1}{2\pi f_c G_{real} C_2 k} \quad (9)$$

$$C_1 = C_2(k^2 - 1) \quad (10)$$

$$R_2 = \frac{k}{2\pi f_c C_1} \quad (11)$$

The value of C2 must be adopted. Equation (4) is the phase, in degree, of the open-loop transfer function without controller at the desired cut-off frequency. Equation (5) is the gain of the same transfer function at the desired cut-off frequency. Equation (6) is the real gain obtained in (5). Equation (7) is the phase that the controller must compensate. Equation (8) is the k-factor of the current controller. It is a factor used in the procedure to obtain the parameter of the controller. Equations (9) to (11) are the computation to obtain the parameters of the controller.

The discretization of the controller is given by (12).

$$C_i(z) = Z\{C_i(s)\} = C_i(s)|_{s=\frac{T_s}{1-z^{-1}}} \quad (12)$$

where *Ts* is the sampling period and *Z* is the Z-transform.

The result of (12) is a z-domain transfer function given by (13).

$$C_i(z) = \frac{b_0+b_1z^{-1}+b_2z^{-2}}{a_0+a_1z^{-1}+a_2z^{-2}} \quad (13)$$

The coefficients of the digital current controller is given by the following equations.

$$\beta = 4R_1R_2C_1C_2 + 2T_sR_1(C_1 + C_2) \quad (14)$$

$$b_0 = \frac{{T_s}^2+2T_sC_2R_1}{\beta} \quad (15)$$

$$b_1 = \frac{2{T_s}^2}{\beta} \quad (16)$$

$$b_2 = \frac{{T_s}^2-2T_sC_2R_1}{\beta} \quad (17)$$

$$a_0 = 1 \quad (18)$$

$$a_1 = \frac{-8R_1R_2C_1C_2}{\beta} \quad (19)$$

$$a_2 = \frac{4R_1R_2C_1C_2-2T_sR_1(C_1+C_2)}{\beta} \quad (20)$$

The current reference collected from the CPT is given (21).

$$i^*_{statcom(A,B,C)} = \frac{\langle\hat{v}_a i_a\rangle+\langle\hat{v}_b i_b\rangle+\langle\hat{v}_c i_c\rangle}{\|\hat{v}_a\|^2+\|\hat{v}_b\|^2+\|\hat{v}_c\|^2} \quad (21)$$

Where $\hat{v}$ is the unbiased integral, given by (22).

$$\hat{v}(t) = v_{\int}\ (t) - \bar{v}_{\int}\ (t) \quad (22)$$

More details about (21) and (22) care found in [26].

IV. Case Study

The system presented in Fig. 1 was simulated in Matlab/Simulink. Tab. I presents the parameters of the case study.

TABLE I. PARAMETERS OF THE CASE STUDY

Parameter	Value
PCC Line-to-Line RMS Voltage	220 V
PCC frequency	60 Hz
Vdc	1000 V
L	10 mH
R	1 mΩ
Hi	1/10
Fs	30 kHz
fc	3 kHz
φ_d	55°
b_0	1.033954901096934
b_1	0.186375309022809
b_2	-0.847579592074126
a_0	1
a_1	-1.001814949393786
a_2	0.001814949393786

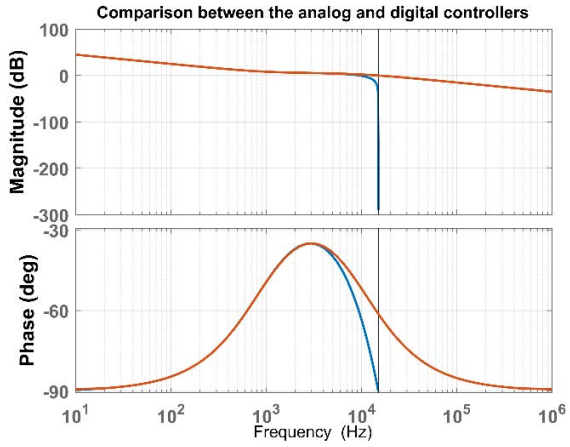

Fig. 2. a comparison between the designed analog and the digital current controller.

Fig. 2 presents a comparison between the designed analog and the digital current controller. The plots are the frequency response of the current controller. At the top, the plot is the magnitude response while the at the bottom, the plot is the phase response. This result shows the efficacy of the discretization through Backward-Euler approximation.

Fig. 3 presents the Bode diagrams for the Closed-Loop transfer function considering the analog current controller. Notice that the cut-off frequency is 3 kHz and the phase margin is 55°, showing that the desired parameters were achieved. Therefore, the current controller is well tuned and the procedure presented in this paper is accurate.

Initially, switches S1, S2 and S3 are off. Therefore, the PCC has the electric grid and the linear load with P=8kW and

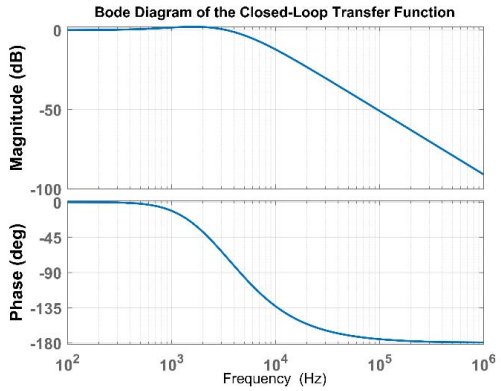

Fig. 3. Bode diagrams for the Closed-Loop transfer function considering the analog current controller.

Q=6kVAr. Fig. 4 presents the three-phase PCC voltage and the three-phase grid current during the initialization of the D-STATCOM. At t=0.15 seconds switch S1 turns on and the D-STATCOM begins to operate. Before t = 0.15 seconds the grid current is sinusoidal and out-of-related to the PCC voltage. After the initialization of the D-STATCOM, the grid current gets in-phase related to the PCC voltage, showing the efficacy of the D-STATCOM in compensating the reactive power of the load. The PCC voltage and the grid current passes through transitory behavior with some oscillations and noise. However, such phenomena are within acceptable levels.

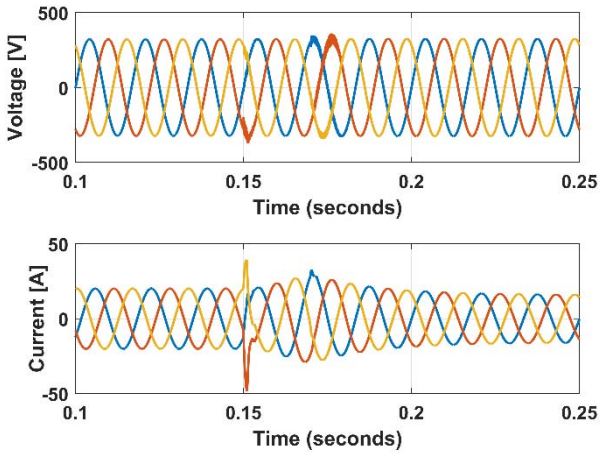

Fig. 4. Three-phase PCC voltage (at the top) and the three-phase grid current during the initialization of the D-STATCOM.

Fig. 5 presents the three-phase load current and the D-STATCOM output current for the same scenario, which is the initialization of the D-STATCOM at t = 0.15 seconds. Before such a moment, the D-STATCOM output current is null. After its initialization and its transitory interval, the D-STATCOM output current reaches 90-degree displacement related to the PCC voltage. The load current keeps unchanged during the initialization of the D-STATCOM, showing that the noises found in the PCC voltage in the previous figure was not harmful to the load.

Fig. 6 presents the current reference signal and the D-STATCOM output current. The D-STATCOM follows the

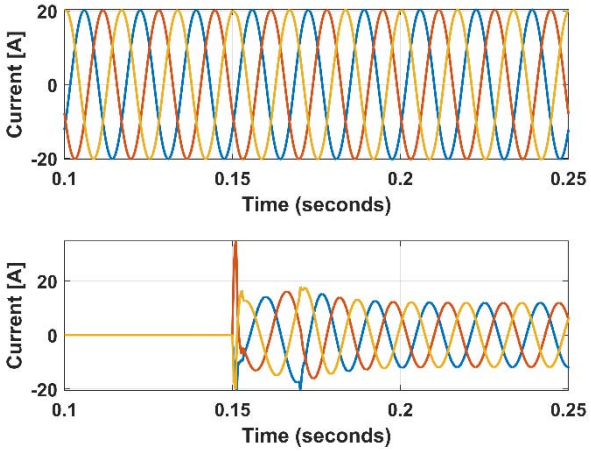

Fig. 5. The three-phase load current (at the top) and the D-STATCOM output current for the same scenario, which is the initialization of the D-STATCOM at t = 0.15 seconds.

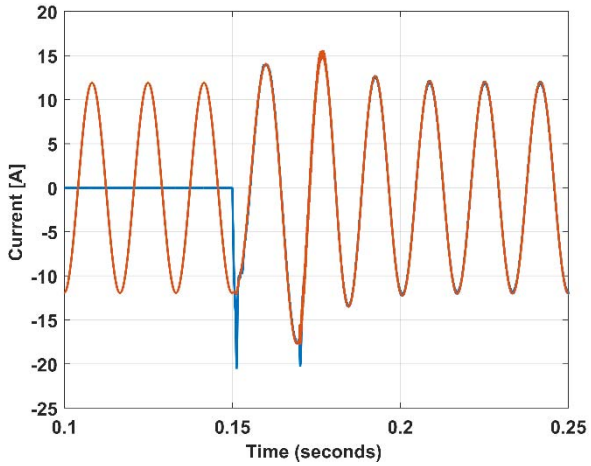

Fig. 6. The current reference signal and the D-STATCOM output current

reference signal with negligible steady-state error. This shows the efficacy of the designed digital current controller.

Fig. 7 presents the three-phase PCC voltage and the three-phase grid current during a load step. At t = 0.8 seconds switch S3 turns on, connecting a linear load to the PCC. This means that more reactive power is being injected into the grid. By looking at the grid current, its amplitude is naturally increased, but the phase displacement between the grid current and the PCC voltage keeps null after the transitory interval. This shows that the D-STATCOM was able to compensate the new amount of reactive power found in the PCC.

Fig. 8 present the current reference signal and the D-STATCOM output current during the same load step. The D-STATCOM output current follow its reference signal with negligible steady-state error.

Fig. 9 presents the three-phase PCC voltage and the three-phase grid current during the connection of the nonlinear load into the PCC. Such connection happens when switch S2 is turned on, at t = 1.35 seconds. The grid current is amplified and results distorted due to the nonlinear behavior of the load. Since the D-STATOM is compensating only reactive power, it is expected that the grid current got distortion.

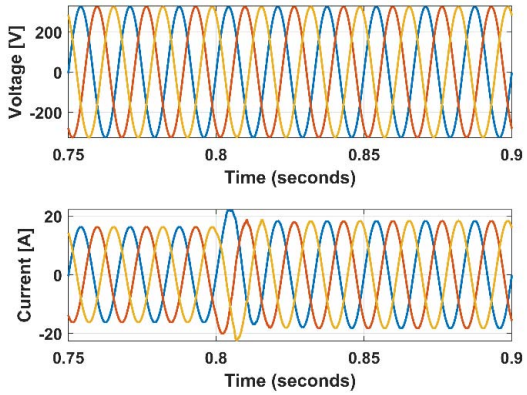

Fig. 7. The three-phase PCC voltage (at the top) and the three-phase grid current during a load step.

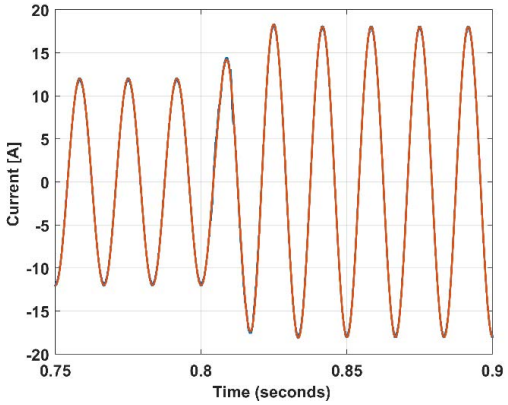

Fig. 8. The current reference signal and the D-STATCOM output current during the same load step.

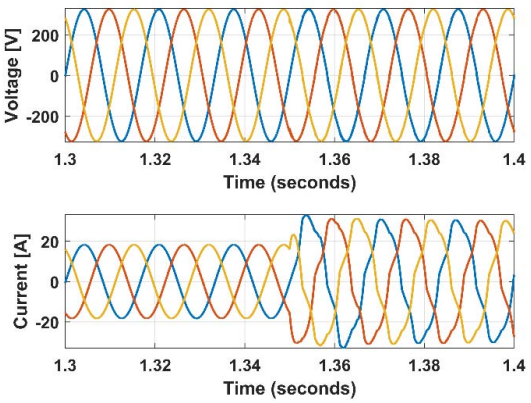

Fig. 9. The three-phase PCC voltage (at the top) and the three-phase grid current during the connection of the nonlinear load into the PCC.

Fig. 10 presents the current reference signal and the D-STATCOM for previous scenario. This result shows two important features of the proposed D-STATCOM, The first is the capability to the D-STATCOM follows its reference signal even for nonlinear load. The second is the ability to the CPT to compute a sinusoidal current from a nonlinear load. Such sinusoidal current has the information of the reactive power produced by the nonlinear load.

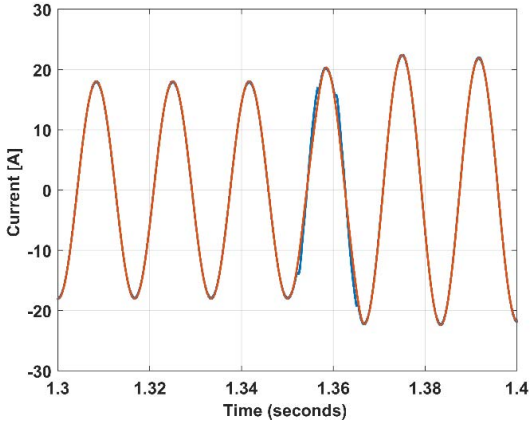

Fig. 10. The current reference signal and the D-STATCOM for previous scenario.

Fig. 11 presents the reactive power in the grid and the DC-link voltage of the D-STATCOM for the whole range of analysis. The reactive power is kept null after the initialization of the D-STATCOM at t = 0.15 seconds. The oscillation in the reactive power at t=0.8 and t=1.35 seconds are due to the load step of the linear and nonlinear load, respectively. It is clear that the reactive power is null even after the connection of the nonlinear load, showing that the D-STATCOM keeps compensating the nonlinear load reactive power even for the distorted grid current. The DC-link voltage is presented in per unit value. Its base value is 1000 V.

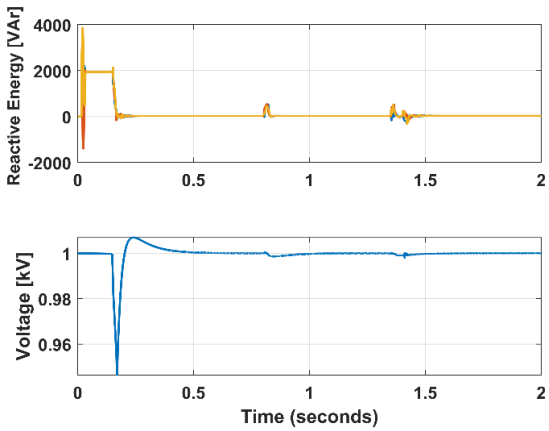

Fig. 11. The reactive power in the grid (at the top) and the DC-link voltage of the D-STATCOM for the whole range of analysis.

V. CONCLUSIONS

This paper proposed a Three-phase D-STATCOM with digital current control strategy in abc-reference frame. The proposal D-STATCOM did not use a PLL and the reactive power was transferred to the grid through controlling the D-STATCOM output current. The current controller has one zero and two poles. The procedure to tune the controller was explained. The Conservative Power Theory was used to

compute the reactive power of the loads. This theory is being broadly used in power electronics applications especially those involving smart-grids. A case study shows the behavior of the D-STACOM during initialization, during load transitions and during steady-state conditions.

A case study with simulation results showed the efficacy of the proposed D-STATCOM. The measured variables did not present neither unpredictable nor oscillatory behaviors. The steady-state errors were negligible. Therefore, the proposed D-STATCOM controlled in abc reference frame is an attractive solution for reactive power compensation in three-phase systems. The simulation files used in this research will be freely available on the author's webpage http://busarello.prof.ufsc.br/.

REFERENCES

[1] C. Steinmetz, "A New Method of Analyzing Armature Reactions of Alternators", *Trans. Am. Inst. Electr. Eng.*, vol. VII, nº 1, p. 434–445, nov. 1890.

[2] P. Rao, M. L. Crow, e Z. Yang, "STATCOM control for power system voltage control applications", *IEEE Trans. Power Deliv.*, vol. 15, nº 4, p. 1311–1317, out. 2000.

[3] H. Akagi, S. Inoue, e T. Yoshii, "Control and Performance of a Transformerless Cascade PWM STATCOM With Star Configuration", *IEEE Trans. Ind. Appl.*, vol. 43, nº 4, p. 1041–1049, jul. 2007.

[4] Y. Neyshabouri, H. Iman-Eini, e M. Miranbeigi, "State feedback control strategy and voltage balancing scheme for a transformer-less STATic synchronous COMpensator based on cascaded H-bridge converter", *IET Power Electron.*, vol. 8, nº 6, p. 906–917, 2015.

[5] Z. Yan, L. Kui, C. Junlin, e L. Jian, "Research on Digital Simulation Technology of H-bridge STATCOM Based on PSCAD/EMTDC and C language Interface", in *2018 IEEE International Power Electronics and Application Conference and Exposition (PEAC)*, 2018, p. 1–6.

[6] Y. Wang, C. Wang, Z. Liu, X. Song, L. Wang, e Q. Jiang, "STATCOM-Based SSCI Mitigation Algorithm for DFIG-Based Wind Farms", in *2018 IEEE International Power Electronics and Application Conference and Exposition (PEAC)*, 2018, p. 1–5.

[7] L. Wang *et al.*, "Reduction of Three-Phase Voltage Unbalance Subject to Special Winding Connections of Two Single-Phase Distribution Transformers of a Microgrid System Using a Designed D-STATCOM Controller", *IEEE Trans. Ind. Appl.*, vol. 54, nº 3, p. 2002–2011, maio 2018.

[8] V. Tummakuri, P. R. Kasari, B. Das, e A. Chakraborti, "D-STATCOM: A study on the NPC multilevel inverter and control strategies", in *2018 International Conference on Power, Instrumentation, Control and Computing (PICC)*, 2018, p. 1–6.

[9] G. Satpathy e D. De, "DC Voltage Reduction in PV connected LV D-STATCOM with In-Phase Series Voltage Injection and Improved Transformer Ratings", in *2018 IEEE 4th Southern Power Electronics Conference (SPEC)*, 2018, p. 1–8.

[10] A. S. Satpathy, D. Kastha, e K. Kishore, "Control of a STATCOM-assisted self-excited induction generator-based WECS feeding non-linear three-phase and single-phase loads", *IET Power Electron.*, vol. 12, nº 4, p. 829–839, 2019.

[11] R. Sajadi, H. Iman-Eini, M. K. Bakhshizadeh, Y. Neyshabouri, e S. Farhangi, "Selective Harmonic Elimination Technique With Control of Capacitive DC-Link Voltages in an Asymmetric Cascaded H-Bridge Inverter for STATCOM Application", *IEEE Trans. Ind. Electron.*, vol. 65, nº 11, p. 8788–8796, nov. 2018.

[12] A. U. Rehman, C. Zhao, e C. Guo, "Coordinated Control Strategy for Transient Performance Improvement of LCC Based HVDC Transmission System with STATCOM Under Weak AC Grid", in *2018 2nd IEEE Conference on Energy Internet and Energy System Integration (EI2)*, 2018, p. 1–6.

[13] V. Pires, A. Cordeiro, D. Foito, e F. Silva, "A STATCOM Based on a Three-Phase, Triple Inverter Modular Topology for Multilevel Operation", *IEEE Trans. Power Deliv.*, p. 1–1, 2019.

[14] Y. Neyshabouri e H. Iman-Eini, "A New Fault-Tolerant Strategy for a Cascaded H-Bridge Based STATCOM", *IEEE Trans. Ind. Electron.*, vol. 65, nº 8, p. 6436–6445, ago. 2018.

[15] G. d S. Neves e J. A. Santisteban, "A comparison between two single-phase static compensator methodologies — PQ theory and state feedback", in *2018 Simposio Brasileiro de Sistemas Eletricos (SBSE)*, 2018, p. 1–6.

[16] P. E. Melin *et al.*, "Study of Reactive Power Compensation Capabilities and LC Filter Design for a Three-Phase Current-Source STATCOM", in *2018 IEEE International Conference on Automation/XXIII Congress of the Chilean Association of Automatic Control (ICA-ACCA)*, 2018, p. 1–5.

[17] P. E. Melin *et al.*, "Study of Reactive Power Compensation Capabilities and LC Filter Design for a Multilevel Three-Phase Current-Source D-STATCOM", in *IECON 2018 - 44th Annual Conference of the IEEE Industrial Electronics Society*, 2018, p. 3640–3645.

[18] L. Maharjan, T. Tajyuta, H. Shinohara, A. Suzuki, e A. Toba, "Control of a 6.6-kV Transformerless STATCOM Based on the MMCC-SDBC using SiC MOSFETs", in *2018 International Power Electronics Conference (IPEC-Niigata 2018 -ECCE Asia)*, 2018, p. 1840–1846.

[19] D. Lu, S. Wang, J. Yao, T. Yang, e H. Hu, "Cluster Voltage Regulation Strategy to Eliminate Negative-Sequence Currents Under Unbalanced Grid for Star-Connected Cascaded H-Bridge STATCOM", *IEEE Trans. Power Electron.*, vol. 34, nº 3, p. 2193–2205, mar. 2019.

[20] H. Li, Y. Guo, J. Xia, Z. Li, e X. Zhang, "Open-circuit fault diagnosis for a fault-tolerant three-level neutral-point-clamped STATCOM", *IET Power Electron.*, vol. 12, nº 4, p. 810–816, 2019.

[21] S. U. Haq, B. Arif, A. Khan, e J. Ahmed, "Automatic three phase load balancing system by using fast switching relay in three phase distribution system", in *2018 1st International Conference on Power, Energy and Smart Grid (ICPESG)*, 2018, p. 1–6.

[22] Z. Guo e L. Li, "Inverter-less Static Synchronous Compensation Based on Three-level AC-AC Converter for Reactive Power and Harmonic Compensation", in *2018 IEEE International Power Electronics and Application Conference and Exposition (PEAC)*, 2018, p. 1–6.

[23] B. Behera e K. C. Rout, "Comparative Performance Analysis of SVC, Statcom UPFC During Three Phase Symmetrical Fault", in *2018 Second International Conference on Inventive Communication and Computational Technologies (ICICCT)*, 2018, p. 1695–1700.

[24] M. H. Alqatamin, M. L. McIntyre, J. Latham, P. Rivera, e N. Hawkins, "Nonlinear Adaptive Control Design for Power System with STATCOM device", in *2018 Annual American Control Conference (ACC)*, 2018, p. 3062–3067.

[25] H. Akagi, E. H. Watanabe, e M. Aredes, *Instantaneous Power Theory and Applications to Power Conditioning*. John Wiley & Sons, 2017.

[26] T. D. C. Busarello, A. Mortezaei, A. Péres, e M. G. Simões, "Application of the Conservative Power Theory Current Decomposition in a Load Power-Sharing Strategy Among Distributed Energy Resources", *IEEE Trans. Ind. Appl.*, vol. 54, nº 4, p. 3771–3781, jul. 2018.

[27] T. D. C. Busarello, J. A. Pomilio, e M. G. Simões, "Passive Filter Aided by Shunt Compensators Based on the Conservative Power Theory", *IEEE Trans. Ind. Appl.*, vol. 52, nº 4, p. 3340–3347, jul. 2016.

[28] T. D. C. Busarello e J. A. Pomilio, "Bidirectional multilevel shunt compensator with simultaneous functionalities based on the conservative power theory for battery-based storages", *Transm. Distrib. IET Gener.*, vol. 9, nº 12, p. 1361–1368, 2015.

[29] T. D. C. Busarello, H. K. M. Paredes, J. A. Pomilio, e M. G. Simões, "Synergistic operation between battery energy storage and photovoltaic generator systems to assist management of microgrids", *Transm. Distrib. IET Gener.*, vol. 12, nº 12, p. 2944–2951, 2018.

[30] T. D. C. Busarello e J. A. Pomilio, "Synergistic operation of distributed compensators based on the conservative power theory", in *2015 IEEE 13th Brazilian Power Electronics Conference and 1st Southern Power Electronics Conference (COBEP/SPEC)*, 2015, p. 1–6.

[31] K. Ogata, *Discrete-time Control Systems*. Prentice-Hall International, 1995.